

FABRICATION OF PATTERNED CARBON NANOTUBE (CNT) / ELASTOMER BILAYER MATERIAL AND ITS UTILIZATION AS FORCE SENSORS

Wenjun Xu¹ and Mark G. Allen^{1,2}

¹School of Polymer, Textile and Fiber Engineering, Georgia Institute of Technology, Atlanta, GA, USA

²School of Electrical and Computer Engineering, Georgia Institute of Technology, Atlanta, GA, USA

ABSTRACT

This paper reports a room-temperature fabrication process for production of localized regions of highly-loaded carbon nanotube (CNT) networks within the surface layers of polydimethylsiloxane (PDMS). These bilayer micro-structures are formed by electrophoretic deposition (EPD) of CNTs into a patterned mold, followed by a transfer-micromolding step. The fabricated CNTs/PDMS bilayer exhibits flexibility, maintains a high local CNT concentration while eliminating issues associated with dispersion and bulk rheology, and preserves the spatial orientation of the original EPD pattern. The use of the material is demonstrated in piezoresistive strain and transverse compression force testing, and is characterized for sensor applications.

KEYWORDS

Micropatterning; Electrophoretic deposition; Carbon nanotubes; Flexible strain sensor; transverse force sensor

INTRODUCTION

The unique structural and electrical properties of carbon nanotubes (CNTs) enable a wide range of smart structure applications. Multiple efforts have been made to incorporate this versatile material into microelectronics [1]. However, the relatively poor processability of this material hinders its widespread use. To integrate this high aspect ratio nanomaterial into miniature systems, precise micro/nano manipulation is required. Multiple approaches to micropatterning of CNTs for controlled integration into microsystems have been considered, including: pre-patterning of catalyst followed by high temperature growth [2]; assembly of CNTs across electrode gaps via dielectrophoresis [3] or AFM positioning; and polymer assisted layer by layer (LBL) self-assembly on microstructures [4]. Issues remaining with these strategies include high temperature processing, slow self-assembly process, and potential introduction of impurities into CNT. Purification of CNTs is critical for reliability and reproducibility of the device on which they rely. Precise control of the thickness and morphology of CNTs are also important for quantitatively studying their properties in microsystems and optimizing the device performance.

Electrophoretic deposition is an attractive bottom-up strategy for CNT manipulation due to its capability of rapidly and uniformly depositing purified CNTs onto large substrates with controlled mass at room temperature [5]. Furthermore, CNT-elastomer nanocomposites are

especially attractive when the microstructure bearing CNTs undergoes mechanical deformation, since the combined architecture can benefit both from the elasticity of polymers and the unique electrical and piezoresistive properties of CNTs [6]. The stretchable system is capable of covering arbitrary curved surfaces and moving objects, which enables applications in low-cost, bio-compatible and flexible physical sensors. However, most reported CNT-elastomer systems are based on bulk composites where CNTs are dispersed throughout the polymer. This approach consumes large amounts of CNTs, and has the further challenge of ensuring excellent dispersion of CNTs in viscous solutions. The bulk composite approach also may not enable applications where both CNT and CNT-free regions are required within the elastomer.

This work exploits a water-based, room-temperature EPD step to rapidly assemble CNTs into pre-patterned 2-D/3-D microstructures [7], followed by transfer micromolding of the CNTs into a PDMS film. The CNT micropatterns are thereby embedded in the uppermost layers of the molded PDMS film, while simultaneously maintaining their original geometric layout. The fabrication process, resultant CNT-PDMS bilayer films, and characterization of the films as transduction materials for piezoresistive strain sensors are described.

EXPERIMENTAL

Detailed description of the experiments and discussion of micropatterning of CNTs on various microstructures by EPD have been reported previously by us [7]. Briefly, multi-wall CNTs (Nanostructured & Amorphous Materials, Inc. 95+ %) were acidified in a mixture of concentrated sulfuric acid and nitric acid to facilitate the EPD process. Three geometric types of microstructures, interdigitated gold microelectrode arrays, silicon microchannels and a SU-8 circular microwell array, were fabricated on silicon substrates as templates for EPD. The microstructure-bearing substrates (anode) and a copper counterelectrode (cathode) were immersed in the CNT aqueous dispersion (0.1mg/ml) and electrically energized with an electric field of 20V/cm for various times (Fig. 1a). The deposited mass can be determined by the time duration of a given microstructure/dispersion deposition [7, 8].

The fabricated micropatterns of the CNT were then transferred to a PDMS matrix by pouring liquid PDMS oligomer into the CNT micropatterns, curing it at 120 °C for 40min, followed by demolding the PDMS (Fig. 1b-c).

Upon demolding, the CNT layer is transferred to the PDMS film.

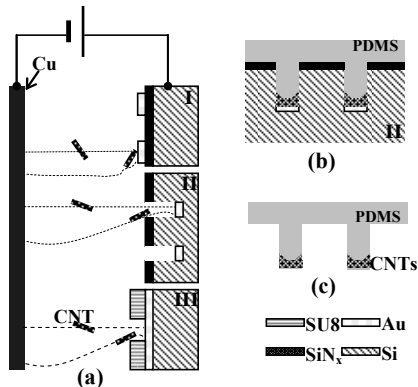


Figure 1: Process flow for CNTs microstructures (I, interdigitated gold microelectrode array; II, silicon micro-channel array, and III, SU-8 microwell array) and transfer micromolding (b & c).

Scanning Electron Microscopy (SEM) (Zeiss, Ultra60) was utilized to study the morphology of the CNT micropatterns and CNT-PDMS bilayer structure. Energy-dispersive X-ray spectroscopy (EDS) was used to characterize the elemental composition of the topmost surface of the CNT/PDMS microstructures.

To demonstrate piezoresistivity of the produced CNT/PDMS composite, the relationship between resistance and transverse compression force of the flexible microstructure was studied. A sample of film was placed on an electronic balance on a probe station. Two probes were placed 800um apart on a 40 um wide testing CNT/PDMS microline. An Agilent 34401A 6.5 digit multimeter was connected to the two probes to determine the resistance of the microline. The transverse compression force was applied through a 70um-wide probe at the middle of the testing microline. During testing, the two probes for the resistance readout were carefully adjusted each time after the force was applied to ensure good contact with the CNTs layer to minimize changes in the contact resistance. The compression force was read from the electronic balance supporting the sample.

The resistance change due to axial strain was studied in a Mini ElectroForce® 3100 Test Instruments (Bose, USA). A 200um wide and 1000um long CNT/PDMS bi-layer microline with two 2mm*2mm CNT pads at the two ends was suspended within a metal-coated plastic frame with a 1mm central gap. The samples were O₂ plasma treated (except the CNT area) to increase the bonding with epoxy-based glue. The two ends of the sample were then coated with a 90nm titanium film and glued to the metal layer on the frame with silver epoxy with the CNTs layer facing down to the frame. An epoxy-based glue was further applied to fully bond the sample to the frame. Two such frames with different stiffnesses were employed for the

sample packaging. The samples prepared for testing are referred to below as sample 1 (less stiff but rigid frame) and sample 2 (stiffer frame). Monotonic tensile strain testing was performed by a WinTest® digital control system. The resistance R was obtained through the multimeter connected to the frame. The gauge factor, G, of the piezoresistive film, was calculated by equation 1:

$$G = \frac{R - R_0}{\epsilon} \quad (1)$$

where R₀ is the initial resistance and ε is the uniaxial strain imparted to the sample by the measurement instrument. .

RESULTS AND DISCUSSION

Three different 2-D/3-D CNT micropatterns were successfully generated on the microstructures with controllable layer thickness ranging from 133nm (Fig. 2a) to several micrometers (Figure 2b & 2c) in less than 4 min. the patterns consist of 3 to tens of layers of the CNTs since the tube diameter is approximately 50 to 80nm. When no substantial topography was present in the microstructures,

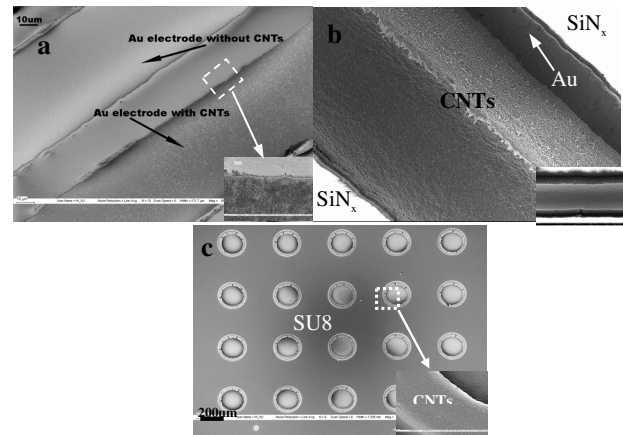


Figure 2: SEM images of CNTs micropatterns in (a) I, microelectrodes, (b) II, Si microchannels and (c) III, SU-8 microwell array

the resultant CNT micropatterns typically assembled only onto those conductive metal areas which were electrically active (Figure 1a). The negatively charged CNTs were neutralized and aggregated when reaching those surfaces. Figure 1b shows that the CNTs can form a highly-dense, packed block inside the silicon microchannels. As observed in Figure 1c, CNTs assembled conformally around the microwell inner surface and in addition generated a 20um wide circular belt framing the well opening, thereby creating a continuous 3-D coating in each isolated microwell. The observation indicates that under these conditions, the deposition of CNTs is in accordance with the conformal coating nature of the EPD process.

An enlarged SEM image shows that the CNTs close to the sidewall of the microchannel tend to align parallel with

the channels (Figure 3). CNTs have been reported to align perpendicular to the electrode substrate (i.e., parallel to the external field lines) under very high electric [9] and magnetic fields [10]. The reason for the observation here at low DC field (20V/cm) is unclear now but could be attributable to directional re-arrangement of the tubes under distorted and concentrated DC field near the sidewalls.

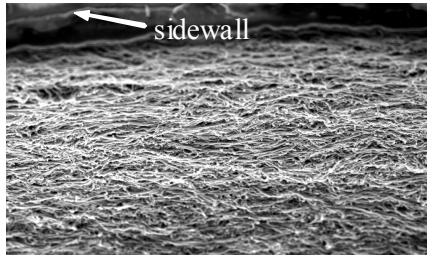


Figure 3: Alignment of CNTs in silicon microchannel

The SEM images in Figure 4 show that the transfer micromolded CNT pattern exhibits a bi-layer structure. A thin, highly-CNT-loaded PDMS layer sits atop a CNT-free PDMS bulk layer which was molded from the original

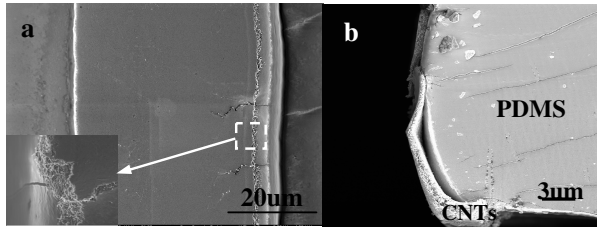


Figure 4. SEM images of CNTs/PDMS bilayer microline (a) top view, and (b) cross section view.

silicon microchannel structure. The thickness of the CNT layer varies from 800nm in the center to 4µm near the edge due to the non-uniform electric field distribution inside the silicon microchannel.

The element spectrum of the surface of the CNT layer obtained from EDS matches that of the pure PDMS (Figure 5). This result, together with the SEM (Figure 4a) confirms that the top CNT layer is in-situ encapsulated by an

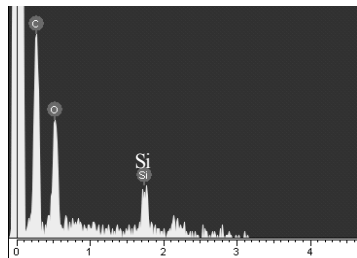


Figure 5: EDS of the top surface of CNTs/PDMS microline

ultra-thin film of PDMS. This is useful for isolation of CNT from the outer environment which may give a more stable device performance.

The transverse compression force sensitivity of the

fabricated CNTs/PDMS bilayer micro-line was shown in Figure 6. The structure exhibits piezoresistive behavior and the resistance increases along with the increase of the transverse compression. Under 7.68mN force, the resistance increased significantly from 0.23MΩ to 2.9MΩ. The resistance was restored to the value of 0.25 MΩ when

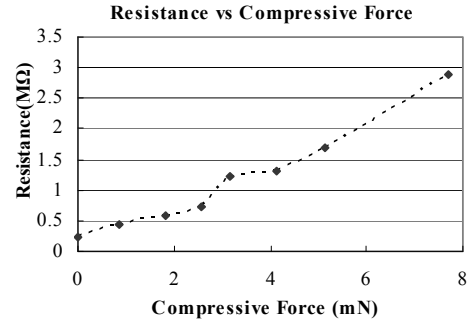


Figure 6: Compressive Force vs. Resistance on CNTs/PDMS bilayer microline

the load was released. A cyclic force study (Figure 7) on the same microline indicates that the resistance can always be restored to the value that is close to the original value during testing. This confirms that the increment of resistance is not due to damage of the CNTs/PDMS conductive layer. Studies have shown that a CNT undergoing mechanical deformation such as bending, flattening, or twisting exhibits changes in its electronic transport properties [11]. In the present study, the order of magnitude increase in the resistance during loading could be attributable to this effect and/or standard percolation-based effects, and is under study.

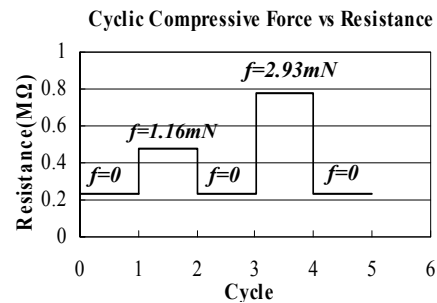


Figure 7: Cyclic Force vs. Resistance on CNTs/PDMS microline

The piezoresistive response of the CNT/PDMS bi-layer microstructure was further characterized in a strain sensor application. As shown in Figure 8, the sample S1 (mounted on a thinner frame) and S2 (mounted on a stiffer frame) both gave a similar curve profile (Figure 8). The gauge factors show similar trends of monotonic increase under higher strain. Under small strain (<2.5%), the samples exhibited gauge factors (G) between 20 and 31. The G increased to between 73 and 162 for larger applied strains ranging from 2.6% to 14% (Figure 10). After load were released, measured resistances went back to 0.42MΩ for

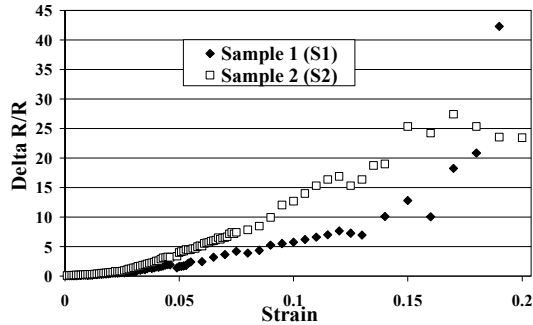


Figure 8: Gauge factor measurement of CNTs/PDMS microlines with thinner (F1) and thicker (F2) loading frames.

S2 and $0.59\text{M}\Omega$ for S1 right after the load was released, which is close to the original value of $0.38\text{M}\Omega$ and $0.462\text{M}\Omega$, respectively. The CNT/PDMS bi-layer material exhibits much higher strain sensitivity than the traditional metal foil strain sensor ($G=2.1$). The variation of gauge factors obtained from the two samples could be attributed to the intrinsic difference between the two samples (concentration of the CNTs, etc.,) or the different stiffness of the two frames.

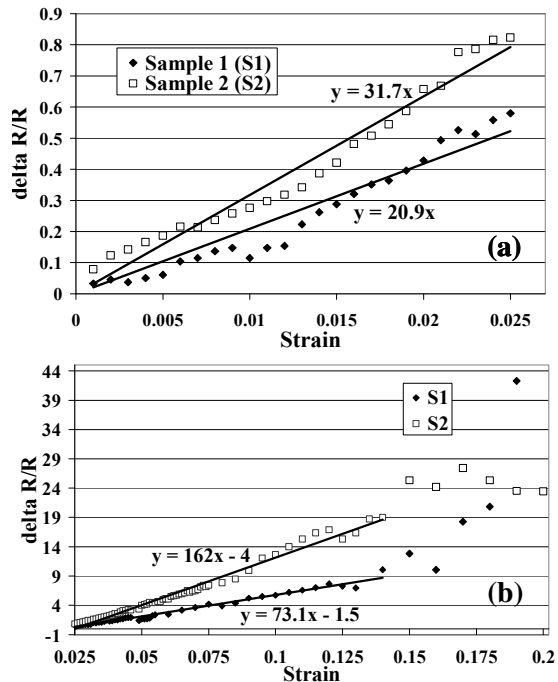


Figure 9: Piezoresistive response of CNT-PDMS microlines under (a) small strain (0~2.5%) and (b) higher strain (2.5~14.5%)

CONCLUSIONS

Various 2D/3D micropatterns of CNTs have been successfully achieved through the facile bottom-up strategy of EPD. The resultant CNT/PDMS bi-layer flexible structure exhibits high sensitivity to both the transverse compressive force and tensile force. This flexible bilayer micro-architecture may lead to potential applications in

sensing/monitoring local pressure/structural change in tissue or micro-fluidic systems, as well as functionalized flexible 3-D microsystems with hybrid multilayer materials.

ACKNOWLEDGEMENTS

The authors would like to thank Professor Oliver Brand and Ms. Maxine A McClain for kind assistance with the experimental setup of resistance- force/strain measurement.

REFERENCES

- [1] P. Sharma, P. Ahuja, "Recent advances in carbon nanotube-based electronics", *Mater. Res. Bull.*, vol.43, pp. 2517–2526, 2008.
- [2] G. Jeong, E. Campbell, "Effect of catalyst pattern geometry on the growth of vertically aligned carbon nanotube arrays", *Carbon*, vol. 47, pp. 696-704, 2009.
- [3] S. Sorgenfrei, I. Meric, K. L. Shepard, et al., "Controlled dielectrophoretic assembly of carbon nanotubes using real-time electrical detection", *Appl. Phys. Lett.*, vol. 94, pp. 053105 (1-3), 2009.
- [4] K. J. Loh, N. A. Kotov, et al., "Multifunctional layer-by-layer carbon nanotube–polyelectrolyte thin films for strain and corrosion sensing", *Smart Mater. Struct.*, vol.16 pp. 429-438, 2007.
- [5] R. B. Aldo, S.P.S. Milo, et al., "Electrophoretic deposition of carbon nanotubes", *Carbon*, vol.44, pp.3149-3160, 2006.
- [6] T. Sekitani, Y. Noguchi, K. Hata, et al., "A Rubberlike Stretchable Active Matrix Using Elastic Conductors", *Science*, vol.321, pp.1468-1472, 2008.
- [7] W. Xu, C. Ji, R. Shafer, M. Allen, "Fast and controlled integration of carbon nanotubes into microstructures", in *Proc. Materials Research Society conference*, Boston, Dec. 1-5, 2008, No.:1139-GG03-06.
- [8] M. Guduru, A. Francis, T. A. Dobbins, "Electrophoretic Deposition of Carbon Nanotubes into Device Structures: A Novel Approach to integrate Nanostructures into Microdevices", *Mater. Res. Soc. Symp. Proc.*, 858E, HH13.29.1, 2005.
- [9] C. Ma, W. Zhang, J. Liang, et al., "Alignment and dispersion of functionalized carbon nanotubes in polymer composites induced by an electric field", *Carbon*, vol. 46, pp.706-710, 2008.
- [10] K. Kordas, T. Mustonen, P. M. Ajayan, et al., "Magnetic-Field Induced Efficient Alignment of Carbon Nanotubes in Aqueous Solutions" *Chem. Mater.*, vol.19, pp. 787-791, 2007.
- [11] C. H. Hu, C. H. Liu, S. Fan, et al., "Resistance-pressure sensitivity and a mechanism study of multiwall carbon nanotube networks/poly (dimethylsiloxane composites)", *Appl. Phys. Lett.*, vol. 93, pp.033108-0331083, 2008.

CONTACT

*W. Xu, tel: +1-404-579-4446; w Xu3@mail.gatech.edu